AIAA JOURNAL
Vol. 42, No. 10, October 2004

Hypersonic Pressure, Skin-Friction, and Heat Transfer Distributions on Space Vehicles: Planar Bodies

Amolak C. Jain*
Science and Technology Corporation, Hampton, Virginia 23666
and
James R. Hayes†
U.S. Air Force Research Laboratory, Wright–Patterson Air Force Base, Ohio 45433

An innovative approach is adopted to develop a new engineering method that predicts pressure, skin-friction, and heat transfer distributions on vehicles of arbitrary shape, flying from the hypersonic continuum, through the transitional and free molecular flow regimes. Salient features of the method are that a single algebraic expression for each of the surface quantities (pressure, skin-friction, and heat transfer coefficients) gives values of the surface quantities on sharp- as well as blunt-nosed vehicles. Only the prescribed flight conditions and surface geometry are needed to obtain results on two-dimensional planar or three-dimensional bodies. Included in the current method are rarefaction effects in the transitional regime, viscous–inviscid interaction effects in the hypersonic continuum regime, equilibrium high-temperature gas effects, and three-dimensional effects arising due to noncircular cross sections of asymmetric shape vehicles. The method is validated against the available data from computational fluid dynamics, direct simulation Monte Carlo method, and wind-tunnel and flight data. This engineering method is reasonably accurate, easy to operate, and fast to execute. A brief review of the available engineering codes is made. An attempt is made to explain the underlying ideas in deriving the algebraic expressions for each of the surface quantities and apply them to planar flows. Extension to three-dimensional bodies is made.

Nomenclature

b_{fi}, b_{hi}, b_{pi}	=	bridging functions defined by Eqs. (1a), (2a), and (3a), respectively
C	=	Chapman–Rubesin constant, $\mu_\infty/\mu_w \times T_w/T_\infty$
C_f	=	skin-friction coefficient, $\tau_w/\frac{1}{2}\rho_\infty u_\infty^2$
C_{f0}, C_{f1}	=	coefficients defined in Eq. (2)
C_h	=	heat transfer coefficient, $\dot{q}/\frac{1}{2}\rho_\infty u_\infty^3$
C_{h0}, C_{h1}	=	coefficients defined in Eq. (3)
C_p	=	pressure coefficient, $(p - p_\infty)/\frac{1}{2}\rho_\infty u_\infty^2$
C_{p0}, C_{p1}, C_{p2}	=	coefficients defined in Eq. (1)
c	=	modified Chapman–Rubesin constant, $\mu(T^*)/\mu_\infty \times T_\infty/T^*$
c^*	=	coefficient in Eq. (10)
H	=	total enthalpy
L	=	characteristic length
M_1 or M_∞	=	free stream Mach number
m	=	defined in Eq. (4)
P	=	ratio of wall pressure with viscous effects to free stream pressure
Pr	=	Prandtl number
P_0	=	ratio of inviscid wall pressure to free stream pressure
p	=	pressure per unit area
p^*	=	coefficient in Eq. (9)
$\dot{q}$	=	heat flux rate per unit area
$Re_{x\infty}$, Re_{0x}	=	freestream Reynolds number, $\rho_\infty u_\infty x/\mu(T_\infty)$ and $\rho_\infty u_\infty x/\mu(T_{e0})$
Re_0	=	stagnation Reynolds number, $\rho_\infty u_\infty L/\mu(T_{e0})$
St	=	Stanton number, $\dot{q}/\rho_\infty u_\infty(H_\infty - H_w)$
s^*	=	coefficients defined by Eq. (11)
T	=	temperature
T_{e0}	=	freestream stagnation temperature, $T_\infty\{1 + [(\gamma - 1)/2]M_\infty^2\}$
T_{wall}	=	wall temperature
T^*	=	reference temperature defined by Eq. (13)
t_{w0}	=	ratio of wall to stagnation temperatures
u	=	tangential component of velocity
x	=	distance along the flat plate or a wedge
y	=	distance normal to the flat plate or a wedge
α	=	angle of incidence or semivertex angle of the wedge
γ	=	ratio of specific heats
δ	=	boundary-layer thickness
δ^*	=	displacement thickness
θ	=	angle that the tangent at a point on a body makes with the freestream
κ	=	thermal conductivity
λ	=	defined in Eq. (4)
μ	=	viscosity coefficient
τ	=	viscous shear stress
$\bar{\chi}$	=	viscous interaction parameter, $M_\infty^3\sqrt{C}/\sqrt{(Re_{x\infty})}$

Subscripts and Superscripts

con	=	value under hypersonic continuum conditions
fm	=	value under free molecular flow conditions
w or wall	=	value at the wall conditions
1 or ∞	=	value at freestream conditions
$*$	=	reference condition

Received 24 July 2003; revision received 2 June 2004; accepted for publication 2 June 2004.

*Senior Research Scientist. Associate Fellow AIAA.
†Aerospace Engineer, Vehicle Integration Branch, AFRL/VAAA.

Introduction

CURRENTLY NASA and various organizations in the Department of Defense (DOD) are deeply engaged in developing space vehicle configurations that can achieve the missions of the respective organizations. NASA is developing a multiple-purpose space crew vehicle to ferry cargo and human beings to and from

the moon and Mars. The U.S. Air Force (USAF) is actively pursuing several projects leading to the development of a space vehicle that can serve as a platform for surveillance and to deliver cargo on demand at any point on the globe within a 2-h period. The USAF vehicles are high lift-to-drag slender vehicles, which due to excessive growth of the boundary layers give rise to induced pressure that feeds back to the boundary layers and significantly increases surface pressure level and heat fluxes.

To arrive at a preliminary design of a space vehicle that is economically viable, reliable, and safe, a designer has to iterate thousands of time steps among various engineering codes for predicting aerodynamic and thermal loads, heat conduction, mechanical and thermal stresses in multilayer and multistructured thermal protection materials and in the primary structure, and trajectory analysis. In the case of the X-43A vehicle, the main vehicle is integrated with a scramjet engine. The mentioned codes have to be executed along with a propulsion code. To save money and time, the engineering codes for various disciplines should be highly accurate, be quick to execute, and be capable of estimating the effects of various performance parameters. The engineering method developed in the present investigation is called the Hypersonic Aerodynamic and Thermal Loads Analysis Program (HATLAP). The HATLAP method has attained these objectives.

A space vehicle has to fly in the upper free molecular flow region of the atmosphere for a sustained period of time. Here the vehicle experiences some drag due to the infrequent collision of molecules and consequently loses altitude. Small hydralzine rockets raise its altitude to the desired position. They also suffer from accumulated heat, which has to be alleviated by mechanical means. Methods of evaluating drag and heating in the free molecular regime are well established in the literature.

As the vehicle reenters the atmosphere, it encounters the rarefied regime, where the mean free path is comparable to or less than the characteristic body length. Methods for predicting surface quantities in the rarefied regime have gained importance because the USAF missions of surveillance and quick cargo delivery require that the vehicle stay in this regime for a sustained period of time. In the rarefied regime, lift is slightly increased but drag is significantly increased, with the result that lift-to-drag is markedly decreased. Here, because of rarefaction, a thick shock wave merges smoothly with a thick viscous layer near the surface of the vehicle, forming a merged layer regime. Jain,[1] Jain and Dahm,[2] Jain and Adimurthy,[3,4] Jain,[5] and Jain and Kumar[6] investigated the merged layer regime by using the full or truncated Navier–Stokes equations with slip and temperature jump conditions. As the vehicle descends, the thick shock wave touches the viscous layer near the surface, forming a viscous shock layer (VSL), which can be investigated by integrating the truncated Navier–Stokes equations with slip effects through the shock wave.[7,8] The continuum approaches have succeeded in penetrating the rarefied regime only up to a certain extent. The entire rarefied and free molecular regimes have been successfully investigated by the direct simulation Monte Carlo (DSMC) method.

Engineering estimates of the surface quantities in the rarefied regime have been made by Potter and Peterson.[9] Based on the experimental, DSMC and free molecular flow results on spheres, they obtained general expressions for pressure and shear stress distributions on blunt and quasi-axisymmetric bodies. Their predictions agreed reasonably well with the DSMC results on spheres, Aeroassist Flight Experiment (AFE) vehicle and 5-deg sphere cones. However, it is doubtful whether Potter and Peterson's method[9] can be used on slender bodies with sharp leading edges.

In the hypersonic continuum regime, induced pressure due to viscous–inviscid interactions, real-gas effects, and entropy-layer effects due to shock wave curvature exercise significant effects on the growth of boundary layers and surface quantities. Peak heating occurs in the continuum regime. Widely used engineering methods are HABP,[10] MINIVER[11] (miniature version of the JA70 aerodynamic heating computer program), aeroheating,[12–14] and INCHES.[15] No attempt is made here to give a complete bibliography; only a few references are described to point out their merits and limitations.

The HABP[10] is primarily meant for calculating vehicle aerodynamic parameters. There are 17 options for pressure distributions and 10 options for shadow methods. An empirical formulation, derived by Bertram and Blackstock[16] and White[17] for viscous–inviscid interaction effects on pressure distribution, is also included. Skin-friction options include the Eckert reference enthalpy method for laminar flows and the Spalding–Chi method for turbulent flows, and heat transfer is calculated by modified Reynolds analogy. Considerable ingenuity and experience are needed to make the correct choice of method to predict accurately the aerodynamics of the vehicle by the HABP procedure.

The purpose of the MINIVER[11] code is to calculate the inviscid flow conditions at the edge of the boundary layer and then to calculate heat fluxes by a Reynolds analogy (one of several available forms) factor along with the Eckert reference enthalpy concept. To calculate an inviscid flow, elements of the vehicle are approximated by either a wedge for a two-dimensional surface or by a cone for an axisymmetric surface. For cones and wedges, this program gives entropy behind attached shock waves and the surface pressure. For surface angles at which the shock is detached from the cone or the wedge, a normal shock and modified Newtonian surface pressure are assumed. When entropy behind the shock and surface pressure are used as independent variables in the Mollier diagram and isentropic gas relations, other thermodynamic and dynamic quantities are calculated to provide inputs for calculating the boundary-layer skin friction and the heat transfer. Several well-known formulations of predicting heat fluxes for specialized regions such as stagnation points, swept cylinders, reattachment heating, etc., for both laminar and turbulent flows are also given. Wurster et al.[18] compared the results from MINIVER,[11] aeroheating,[13,14] and INCHES[15] codes with computational fluid dynamics (CFD)/wind-tunnel/flight data and found that the MINIVER[11] code has a limited range of applications. From the results of Wurster et al.,[18] it can be observed that, under certain conditions, results from the MINIVER[11] code do not agree qualitatively or quantitatively on the spherical portion of the sphere–cone body when compared with CFD results; however, agreement is good on the conical portion of the sphere–cone. This may be due to that the entropy level behind the normal shock along with the choice of surface pressure distribution may not represent the realistic situation. Three-dimensional effects in the solution of the boundary-layer equations are incorporated by the Mangler transformation, which is valid only for bodies with circular cross sections. Lewis and Sliski[19] applied the MINIVER[11] code on vehicles with noncircular cross sections and with large flat areas exemplified by lifting reentry vehicles. They found that the MINIVER[11] code is unsuitable for this configuration. In spite of these drawbacks, the MINIVER[11] code is widely used in federal agencies and industries. With correct choice of shock shape, pressure, and effective characteristic length extracted from wind-tunnel experimental data or by running Euler's code for each of the prescribed conditions at trajectory points, correct boundary-layers edge conditions can be obtained, and the MINIVER[11] code may give preliminary results of surface quantities for designing the space vehicles. Thus, it is clear that considerable experience is needed to execute the MINIVER[11] code.

Several aeroheating codes for asymmetric or symmetric bodies with and without angles of attack are available. These codes essentially depend on the Cooke analogy[20] that reduces the flow problem on a three-dimensional body, with or without an angle of attack, to an axisymmetric body at zero angle of attack. For this purpose, inviscid flow equations are solved with prescribed surface pressure distribution on the given three-dimensional body, and the length of the inviscid surface streamlines and the streamline metric coefficient are calculated. The length of the streamline from the stagnation point of the given body is taken as the distance from the stagnation point on the axisymmetric body whose radius is equal to the corresponding metric coefficient. The boundary-layer equations on the axisymmetric body are solved by an approximate method to give skin-friction and heat flux distributions, or the local skin friction on the axisymmetric body is calculated by using the flat plate Blasius skin-friction expression with the Mangler transformation and then

heat fluxes are derived by using one of the several forms of Reynolds analogy with Eckert reference enthalpy concept. Fivel[12] developed an aeroheating code with the Cooke analogy[20] by solving the Euler's equations with eight options for surface pressure distributions. For laminar flows, the Beckwith and Cohen[21] method is used to solve the boundary-layer equations on an equivalent axisymmetric body. For turbulent flows, the modified Reshotko and Tucker[22] integral method is used to calculate skin-friction coefficient. The von Kármán analogy is used to calculate heat transfer coefficient distributions. With judicious choice of the options available, comparison of the results on ogive–cylinder, flat bottom delta wing, and slab delta cases at various angles of attack with the available results is good. The DeJarnette and Davis[13] and Hamilton et al.[14] approach differs from the Fivel[12] approach in that they use Maslen's[23] method for calculating the inviscid flow and mass balancing procedures for local entropy effects on surface heating. Also, the heat transfer is calculated on an equivalent axisymmetric bodies by using approximate methods. Wurster et al.[18] found reasonably good agreement of the predicted results from the DeJarnette and Davis[13] and Hamilton et al.[14] method with CFD results on sphere–cones at various angles of attack.

Zoby and Simmond[15] use a modified Maslen's[23] technique in the INCHES[15] code to solve the inviscid flow to get better definition of inviscid surface properties. The method is applied to zero-angle-of-attack flow over ellipsoids, paraboloids, hyperboloids, and sphere–cones. Variable entropy effects are included by using local inviscid properties located a boundary-layer thickness away from the body surface. A modified Blasius skin-friction coefficient with Reynolds analogy and Eckert reference enthalpy is used to compute local heating rates. For angles-of-attack effects on windward and leeward symmetry planes of sphere–cones, the Cooke analogy[20] is used with shock shape and surface pressure given by equivalent cones. Wurster et al.[18] compared the Reentry F data, VSL3D, aeroheating,[11] and INCHES[14] codes on sphere–cones with and without angles of attack and found that the range of applicability of the INCHES[14] code with respect to angles of attack is limited. Wurster et al.[18] further found that a judicious choice has to be exercised in choosing the shock shape and pressure distribution, as well as the use of a Reynolds analogy factor to predict heat fluxes from flat plate skin friction. It is necessary that the user must understand the applicability and accuracy of the options to the actual flowfield physics of the vehicle under consideration. The user should also understand the restrictions imposed on each method and their regions of applicability.

The Cooke analogy[20] assumes small crossflow velocity in the inviscid flow at the boundary-layer edge, that is, divergence of the streamlines in a direction perpendicular to the axial direction and lying in the tangent plane at a point on the body is small. It can be interpreted that the transverse curvature perpendicular to the symmetry plane is small. This condition imposes severe restrictions on the geometry of the body and the extent of the angles of attack. The analysis can give reasonably good results along the line of symmetry in the windward and leeside planes of the body where the surface transverse curvature is negligible. It can also be applied in regions where the streamline curvature in the transverse direction is small or the local curvature of the vehicle geometry in the azimuthal or transverse direction is small. With use of the Cooke analogy,[20] Euler's equations with prescribed surface pressure distributions are solved. The solution gives us streamline length and a metric coefficient to generate an equivalent axisymmetric body. The choice of the pressure distribution to solve the inviscid Euler's equations is not unique. Thompson et al.[24] found that while using the Cooke analogy[20] most engineering codes often used a modified Newtonian formula for pressure distribution, which did not give satisfactory results of heating rates on slender cones even at small angles of attack. There is a need to carry out similar studies for bodies of arbitrary shape. Except for relatively simple bodies such as wedges, cones, spheres, and sphere–cones, it is reasonably difficult to guess the correct form of pressure distribution on bodies of complex configuration and calculate streamline length and metric coefficient for an equivalent axisymmetric body. Thus, the range of application of the Cooke analogy[20] is limited in scope, and it does not give unique results.

Distinguishing Features of the Present Code

First, there is renewed interest in the rarefied regime, mainly because several DOD missions are supposed to fly for a sustained period of time in this regime to achieve their objectives. In the design of vehicles, rarefied flows have so far been almost ignored, mainly because of low-heating rates on vehicles flying in this regime. Although the heat transfer rates are small, the accumulated heat due to long-duration flight in the rarefied regime becomes significant and cannot be ignored. Lift-to-drag ratio is markedly decreased. Several missiles failed to perform in this regime mainly because the designer did not consider the effect of reduced lift-to-drag in this regime. Only the HATLAP method has the capability to predict pressure, skin-friction, and heat transfer distributions; lift-to-drag ratio, and accumulated heat on a vehicle flying in the rarefied regime of the atmosphere with a reasonably high degree of accuracy, in addition to its capability to predict surface quantities in the free molecular and the continuum regimes.

Second, in the hypersonic continuum regime, the engineering codes predict heat fluxes by making use of one of the several forms of Reynolds analogy factor to the Blasius skin-friction expression modified to take account of compressibility of the fluids by using the Eckert reference enthalpy concept. As stated earlier, accurate boundary-layer edge conditions have to be obtained by solving Euler's equations numerically to obtain reasonably accurate results from the Blasius skin-friction expression. Because of the complexity of solving Euler's equations and the large computer time needed to obtain converged solutions, the method can hardly be called engineering method. The HATLAP method predicts aerodynamics (pressure, skin friction) and independently predicts heat fluxes (without the use of any form of Reynolds analogy or Eckert reference enthalpy reference concept) along the trajectory of the vehicle.

The third feature is that, although variable entropy effects are included empirically in aeroheating[13,14] and in INCHES[15] codes, the viscous–inviscid interaction effects, which exercise significant effects on pressure, skin friction, and heat fluxes on slender bodies in hypersonic continuum regime, are not considered in any of the available engineering codes. In the HATLAP method, entropy-layer effects are not considered, but viscous–inviscid interaction effects are rigorously included.

The fourth feature is that, for three-dimensional effects, heat fluxes are calculated by use of Mangler transformation, which is valid only for bodies with circular cross sections and with boundary layers that are thin compared with the characteristic length of the vehicle. Also, the equivalent cone concept is used to give results along the windward symmetry line. The INCHES[14] code gave results only on limited body shapes, such as ellipsoids, paraboloids, and hyperboloids at zero angle of attack and in the symmetry planes of sphere–cones at angles of attack. In aeroheating codes,[12–14] Cooke analogy[20] is used for bodies at angles of attack, which should give reasonable results along the windward and leeward symmetry planes and in the neighboring regions provided the transverse curvature of the vehicle in the neighboring region is small. In the HATLAP method, a general procedure is presented to solve for surface quantities (pressure, skin-friction, and heat flux distributions) in every meridian plane of three-dimensional bodies before the separation sets in.

The fifth feature is that the HATLAP method gives reliable information in free molecular, rarefied, and hypersonic continuum regimes. The code gives reasonably accurate results and can be executed sufficiently fast so that one can get real-time results for the entire trajectory of the space vehicle flight.

HATLAP Method Description

An innovative approach is adopted to derive algebraic expressions for predicting surface pressure, skin-friction, and heat transfer

coefficient distributions on space vehicles in the following form:

$$C_p = C_{p0} + C_{p1} \times \sin\theta + C_{p2} \times \sin^2\theta \tag{1}$$

where

$$C_{pi} = C_{pi,\mathrm{con}} + (C_{pi,\mathrm{fm}} - C_{pi,\mathrm{con}}) \times b_{pi}, \qquad i = 0, 1, 2 \tag{1a}$$

Here, b_{pi}, $i = 0, 1, 2$, are called bridging functions,

$$b_{p0} = \left[a\sqrt{Re_0} + \exp\left(-b\sqrt{Re_0}\right)\right]^{-1}$$

$$a = \frac{(\gamma-1)\sqrt{t_{w0}} + \sqrt{2(\gamma-1)}/M_\infty}{(\gamma-1)\sqrt{\gamma/(\gamma+1)}(1.8534 + 4.51 \times t_{w0})M_\infty}$$

$$b = 0.35 + 0.005M_\infty$$

and stagnation point Reynolds number

$$Re_0 = \rho_\infty u_\infty L/\mu(T_{e0}), \qquad t_{w0} = T_{\mathrm{wall}}/T_{e0}$$

$$C_f = C_{f0} \times \cos\theta + C_{f1} \times \sin\theta \times \cos\theta \tag{2}$$

where

$$C_{fi} = C_{fi,\mathrm{con}} + (C_{fi,\mathrm{fm}} - C_{fi,\mathrm{con}}) \times b_{fi}, \qquad i = 0, 1 \tag{2a}$$

$$C_h = C_{h0} + C_{h1} \times \sin\theta \tag{3}$$

where

$$C_{hi} = C_{hi,\mathrm{con}} + (C_{hi,\mathrm{fm}} - C_{hi,\mathrm{con}}) \times b_{hi} \tag{3a}$$

Because of limitations of space, analytical expressions for the bridging functions b_{pi}, $i = 1, 2$, in Eq. (1a), b_{fi}, $i = 0, 1$, in Eq. (2a), and b_{hi}, $i = 0, 1$, in Eq. (3a) are given in Ref. 25. The basic considerations and mathematical approach in developing the HATLAP method are stated separately in later sections. Symbols in Eqs. (1–3) are defined in the Nomenclature. Various quantities appearing in Eqs. (1a), (2a), and (3a) are analytical expressions of Mach number M_∞, Reynolds number Re_0, t_{w0}, γ, and Prandtl number Pr. Only the freestream conditions along the vehicle trajectory and the vehicle geometry are needed for the execution of the present method. The method gives results on planar bodies, on axisymmetric bodies with circular cross sections, and on bluff-nosed bodies with cross-sectional contours varying in shape and size. In particular, it is easy to see for the flow on a flat plate, described by $\theta = 0.0$, that $C_p \propto (1/\sqrt{x})$, where x is the characteristic length defined as the distance from the leading edge of the flat plate. Note from Eqs. (1–3) that C_p depends on the viscous effects represented by Reynolds number Re_0 and on the temperature ratio t_{w0} in the hypersonic continuum and in the rarefied regimes. The viscous and wall temperature effects on pressure distribution become more significant in the rarefied regime than in the continuum regime. The HATLAP method is probably the only engineering method where the effect of wall temperature on vehicle pressure distribution is realized. The effect of different gases in high-altitude atmospheric conditions is represented by an effective value of gamma. The effective value of gamma is the value of gamma in the mixture of inert gases present in high-altitude freestream vehicle flight conditions.

The correct form for the viscosity–temperature relation is important in calculating the stagnation Reynolds number, to arrive at accurate predictions of surface quantities from Eqs. (1–3). When the HATLAP method results are compared with wind-tunnel data, a linear viscosity–temperature law should be used for low freestream temperature conditions in the test section. Most of the DSMC results are derived from the variable hard sphere collision model of Bird.[26] Also, flight data involve high stagnation temperatures in the hypersonic regime. In such cases, the Sutherland viscosity law should be used. In some CFD calculations, based on either the full or the truncated form of the Navier–Stokes equations, square-root viscosity–temperature law is found convenient. When the results from the HATLAP method are compared with the mentioned CFD results, only the square-root viscosity–temperature law should be used. Care must be exercised in choosing proper viscosity–temperature law in getting greatly improved predictions from the HATLAP method. In the HATLAP methods, options for linear, square-root, three-fourth, and Sutherland viscosity laws are included.

Basic Considerations in Developing the Method

First, for $\theta = 0$, Eqs. (1–3) give $C_p = C_{p0}$, $C_f = C_{f0}$, and $C_h = C_{h0}$. They represent pressure, skin-friction, and heat transfer distributions, respectively, on a flat plate. The flow on a flat plate is a fair representation of the flow on a slender body.

For $\theta = 90$ deg, Eqs. (1–3) give

$$C_p = C_{p0} + C_{p1} + C_{p2} \approx C_{p2} \qquad (C_{p2} \gg C_{p0}, C_{p1})$$

$$C_f = 0.0$$

$$C_h = C_{h0} + C_{h1} \approx C_{h1} \qquad (C_{h1} \gg C_{h0})$$

They represent values of the surface quantities at the blunt-body stagnation point. For the part of the body where surface inclination angle θ with the freestream lies between 0.0 and 90.0 deg, surface quantities are essentially composed of contributions from the slender part, C_{p0}, and blunt part, C_{p2}, of the given body and/or by their interference effects, C_{p1}.

Second, the coefficients C_{pi}, $i = 0, 1, 2$, C_{fi}, $i = 0, 1$, and C_{hi}, $i = 0, 1$, in Eqs. (1–3) contain bridging functions, b_{pi}, $i = 0, 1, 2$, b_{fi}, $i = 0, 1$, and b_{hi}, $i = 0, 1$. For $Re_0 \to \infty$, Eqs. (1a), (2a), and (3a) show that b_{pi}, b_{fi}, $b_{hi} \to 0.0$ and, consequently, the expressions for C_p, C_f, and C_h give values of the respective quantities approaching the hypersonic continuum regime. For $Re_0 \to 0.0$, Eqs. (1a), (2a), and (3a) show that b_{pi}, b_{fi}, $b_{hi} \to 1.0$; then, consequently, the expressions for C_p, C_f, and C_h give values of the surface quantities approaching the free molecular flow regime. For values of Reynolds number Re_0 lying between infinity and zero, values of the surface quantities are obtained from the hypersonic continuum regime to the free molecular flow regime.

Third, equilibrium gas effects are introduced by using the algebraic relations for thermodynamic and transport quantities given by Gupta et al.,[27] and viscosity values are taken from the data of Hansen.[28] Within the present approach, it is not possible to include nonequilibrium gas effects on surface quantities because it involves the knowledge of the flowfield with chemical reactions, which can only be obtained by solving the governing equations of the flow (the Navier–Stokes or one of its truncated forms of equations with chemical reactions and with or without wall catalyticity). To obtain the solution of the governing equations is quite tedious and time consuming. Hence, it falls outside the scope of engineering methods.

From the preceding considerations, it is evident that the engineering relations for pressure coefficient C_p, skin-friction coefficient C_f, and heat transfer coefficient C_h as given in Eqs. (1–3) are based on a generic formulation, applicable for bodies of arbitrary shape. The vehicle shape may consist of a spectrum of bodies consisting of planar parts (flat plates, wedges, etc.), axisymmetric parts with circular cross sections (spheres, sphere–cones, hyperboloids, paraboloids, etc.), and asymmetric bodies with noncircular cross sections (ellipsoids, elliptic cones, elliptic hyperboloids, elliptic paraboloids, etc.) or a combination of several symmetric and asymmetric bodies, such as an AFE vehicle. Only the freestream conditions, the wall conditions, and the vehicle geometry need be prescribed to get unique values of C_p, C_f, and C_h at any point on a vehicle of arbitrary shape, flying in the hypersonic continuum, transitional, or free molecular regimes.

Particular emphasis is placed on including salient features of hypersonic flows such as viscous–inviscid interactions, real gas, rarefaction, and three-dimensional effects in the HATLAP method. Pressure is basically an impact event and is not affected much by

whatever is happening at the neighboring points, but heat transfer is a diffusion phenomenon and is affected by the diffusion of heat from the neighboring regions. Thus, three-dimensional effects significantly affect the heat transfer distribution, particularly when compared to their effect on pressure distribution. From fluid mechanical point of view, the three-dimensional effects arise due to longitudinal as well as transverse compression of the surface fluid element and the presence of crossflow velocity. The class of flows where the crossflow velocity cannot be neglected is governed by the three-dimensional form of the governing equations. In the sequel, an analytic procedure for defining surface quantities on three-dimensional bodies within the framework of Eqs. (1–3) is considered in detail. Validity of the HATLAP method is established by comparing the results of the predictions from the HATLAP method on simple bodies and on bodies of complex configuration with the corresponding DSMC, CFD, and wind-tunnel and flight data.

Motivation and Mathematical Approach in Developing the Method

In the early 1960s, Jain and Li[29] developed an analytical procedure of solving the slip-dominated region near the sharp leading edge of a flat plate. During the 1970s, Kumar and Jain[30] Jain and Kumar,[31] Chaudhury,[32] and Mathews[33] developed an analytical procedure of solving the boundary-layer equations with viscous–inviscid interaction effects and with slip and temperature jump boundary conditions on wedges of semivertical angle of θ and obtained analytical expressions for surface quantities C_p, C_f, and C_h, which showed their correct dependence on dimensionless parameters derived from the freestream and the surface conditions. The form of the expressions for C_p, C_f, and C_h in the hypersonic continuum regime is exactly the same as that of the corresponding quantities in free molecular flows.[34] This suggested a procedure of correlating the surface quantities (C_p, C_f, and C_h) in the hypersonic continuum regime to the free molecular flow regime. Similar expressions for C_p and C_f are obtained by Katov et al.[35] This observation led the authors of Refs. 29–33 to modify the bridging functions for C_p and C_f given by Katov et al.[35] and to extend the approach to derive similar analytical expression for C_h.

Conceptually, Katov et al.[35] adopted the approach that the pressure on the forepart of a blunt body from the stagnation point ($\theta = 90$ deg) to the surface inclination angle defined by $\theta = 47$ deg is represented by the modified Newtonian relation, and in the aft part ($\theta > 47$ deg), pressure is given by the tangent cone followed by the tangent wedge approximations. Katov et al. gave expressions for C_p and C_f similar in form to Eqs. (1) and (2), but their bridging functions are different from those used in Eqs. (1–3). Katov et al.[35] obtained the bridging functions in C_p and C_f from extensive computations using either the Navier–Stokes equations or the VSL equations with surface slip conditions for a number of simple bodies and under a wide range of prescribed flight and wall conditions. It was found that the pressure distribution on the forepart of the sphere did not merge smoothly with the tangent cone pressure in the aft part of the sphere. The criterion of changing the tangent cone pressure to tangent wedge pressure in the farther aft part of the sphere is not well defined. Even if it is given, the tangent cone pressure results will not join smoothly the tangent wedge pressure results.

Knox and Jain[36] applied the formulation of Katov et al.[35] to predict pressure distribution on a sharp leading-edge flat plate at zero incidence, where the problem of merging the modified Newtonian pressure predictions with the tangent cone and the tangent wedge pressure values did not arise. Knox and Jain[36] showed that except for the highest Mach number tested, namely, $M_\infty = 20$, the flat plate pressure distributions under both hot-wall and cold-wall conditions exceeded the corresponding values given by the strong interaction predictions of Li and Nagamatsu.[37] Also, the results of skin-friction distribution on the flat plate were not correct qualitatively or quantitatively. The results of C_f distribution on the flat plate from Katov et al.[35] had no physical significance.

With use of the analytical results derived in Refs. 29–33 and with use of the computed results of Katov et al.,[35] Knox and Jain[36] modified the formulation of C_p and C_f in Eqs. (1) and (2) to give quantitatively and qualitatively correct results on slender as well as on blunt bodies. The results of this investigation were presented by Knox et al.[38] in 1993. However, there were certain typographical errors and omissions in the expressions for C_p and C_f presented in Ref. 38. Based on the new data, the present investigators updated the formulation of C_p and C_f, given by Knox et al. Also, the present investigators further extended the same approach to derive an analytical formula for predicting heat transfer coefficient distributions on bodies of arbitrary shape, HATLAP. Validity of the HATLAP method has been established by comparing the predictions from the HATLAP method with the corresponding DSMC, CFD, and wind-tunnel or flight data.

Discussion of Results

Most of the vehicles that the DOD is investigating are slender, high lift-to-drag configurations. Flow on a slender body can ideally be represented by the flow on a flat plate with a sharp leading edge. Mathematically, the tip of a sharp leading edge has no dimensions. In fluid mechanics, a sharp leading edge can be defined whose thickness is less than or equal to the local mean free path. The reality of achieving such a sharp-leading-edge vehicle is not too far from the reach of engineers.

The NASA Ames Research Center has developed an ultrahigh-temperature material with high conductivity called diborides of hafnium or zirconium with a particulate silicon carbide as a second phase. Another class of material is known as lightweight informed micrometeoroid-resistant ceramic, which with a surface treatment, high-efficiency tantalum-based ceramic, can improve catalytic efficiency, surface emissivity, and impact resistance. Recent arcjet tests have shown its applicability to leading edges operating at temperatures above 1900 K (Ref. 39).

Even if it is not possible to realize a sharp leading edge in a fluid mechanical sense, it is possible to have a vehicle with a small blunt edge that can withstand very high temperatures. The effect of the slight bluntness will be realized only up to a few nose radii downstream of the leading edge. The vehicle on the whole will have all of the fluid mechanical characteristics as are possessed by a slender vehicle. As such, the discussion that follows will have a direct application to the design of many of the vehicles under development.

Figure 1 shows the flow on a flat plate with a sharp leading edge at zero angle of attack. Figure 1 shows a kinetic regime spread over a few mean free paths near the sharp leading edge of the flat plate. Farther downstream is the merged layer, followed by the strong and weak viscous–inviscid interaction regimes, bridged by a transition regime. Here, it is presumed that a molecule after striking the tip of the leading edge of the flat plate collides with the molecules downstream of the leading edge. In a physical situation, the molecule after striking the sharp leading edge of the flat plate may collide with the incoming molecule upstream of the leading edge, but for design purposes, the classical model of flow in Fig. 1 is considered adequate. The HATLAP method is capable of predicting the surface quantities from the free molecular flow at the leading edge to the continuum flow far downstream of the leading edge.

For a flat plate, kinetic, merged layer, and viscous–inviscid interaction regimes exist adjacent to each other at a given altitude. In the case of a blunt-nosed or bluff-nosed vehicle, free molecular, rarefied or merged layer, and viscous interaction regimes pass over the nose portion of the vehicle as it descends through the atmosphere during its reentry phase. The HATLAP methodology can analyze these regimes individually on a blunt- or bluff-nosed space vehicle as easily as it can analyze them on a flat plate where the different regimes exist side by side. It is evident that the flow on a slender vehicle is more complex to analyze than the flow on a blunt-nosed vehicle.

Under conditions of the wind tunnels V1G and V2G of the DFVLR Institute for Experimental Fluid Mechanics, Gottingen, Germany, Moss et al.[40] carried out DSMC computations of the flow on a sharp-leading-edge flat plate of 10 cm length. The DSMC computations show that some of the molecules, after striking the tip of the flat plate, collide with the oncoming molecules. Thus the effect of the plate is realized upstream of the tip of the flat plate. The flow

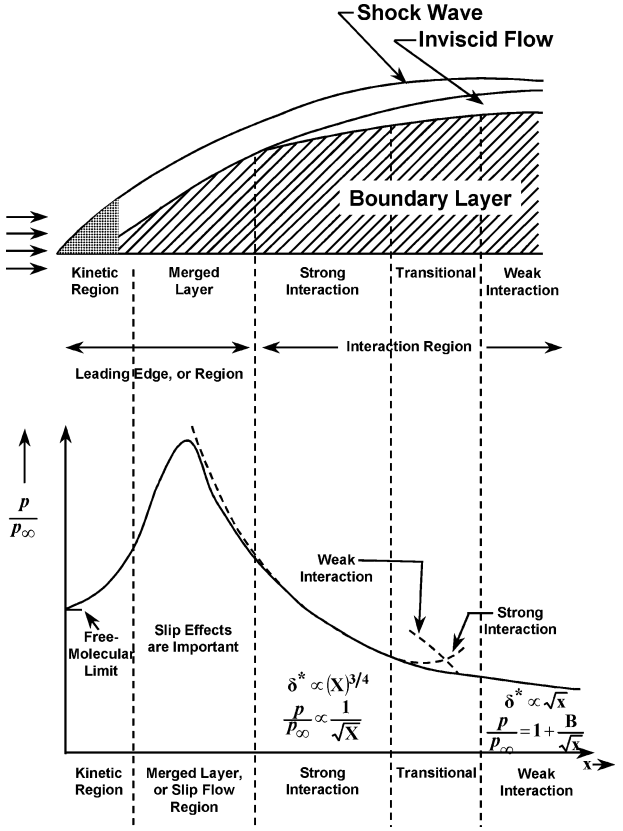

Fig. 1 Classical flow pattern on sharp-leading-edge flat plate.

features on the flat plate are somewhat different from the classical flow pattern represented in Fig. 1.

Li and Nagamatsu[37] obtained similar solutions of the boundary-layer equations with viscous–inviscid interactions on a sharp-edge flat plate at zero incidence for $\gamma = 1.4$, $\mu \propto T$, $Pr = 1.0$, and $t_{w0} = 0.0$, 0.2, 0.6, and 1.0 and derived analytical expressions for C_p, C_f, and C_h. Later, Bertram and Feller[41] carried out extensive computations of similar boundary-layer equations by use of a simple method. Results of Li and Nagamatsu[37] and Bertram and Feller[41] agreed with a high degree of accuracy. Moss et al.[40] computed the flowfield and surface quantities on a flat plate of 10 cm length by the DSMC method using a VHS[26] model of flow under the DFVLR wind-tunnel conditions (V1G and V2G) in Gollingen, Germany, namely, $u_\infty = 1340$ m/s, $\rho_\infty = 5.14 \times 10^{-5}$ kg/m^3, $T_\infty = 8.3$ K, and $T_{\text{wall}} = 383$ K. In this investigation, semi-analytical results of Li and Nagamatsu[37] with some physical approximations and the DSMC results of Moss et al.[40] are compared with the results of the HATLAP method. Figure 2 shows good agreement of pressure coefficient C_p from the present calculations with the Li and Nagamatsu[37] results in the common region of validity. C_p from the present calculations starts from the free molecular flow value at the leading edge of the flat plate and attains a peak value due to multiple collisions of molecules somewhere in the merged layer region and then tends to merge with the strong interaction results of Li and Nagamatsu.[37] In the DSMC computations,[40] a molecule after striking the tip of the sharp leading edge of the flat plate, may travel upstream and collide with the incoming molecules. In the HATLAP method, it is assumed that a fluid particle after striking the tip of the flat plate collides with the molecules downstream of the leading edge. Thus, because of the different modeling of the fluid flow in the DSMC computations and in the HATLAP method, there are quantitative differences in the DSMC and the HATLAP results on the flat plat up to the merged layer regime. The agreement of results from the present method with those of Li and Nagamatsu[37] is reasonably good in the strong interaction regime. Without viscous interaction effects, $C_p = 0.0$ even under hypersonic conditions. Figure 3 shows that the wall pressure rises to about 35 times the freestream pressure due to viscous–

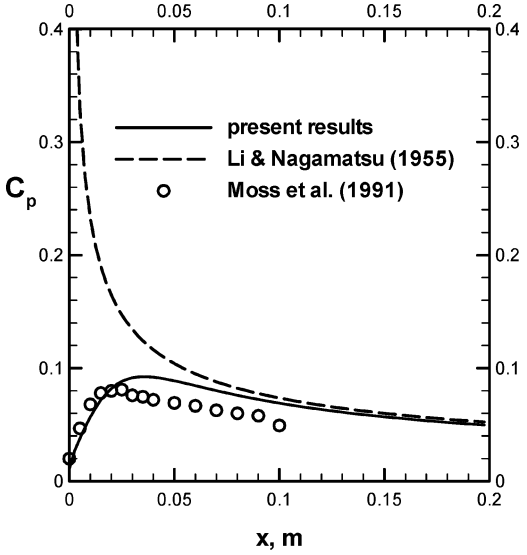

Fig. 2 Comparison of present results with viscous interactions on a sharp-leading-edge flat plate with Moss et al.[40] and Li and Nagamatsu[37] results.

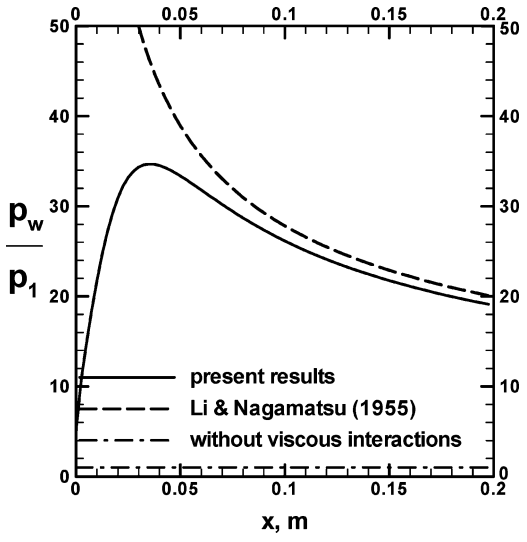

Fig. 3 Comparison of present results with and without viscous interactions on a sharp-leading-edge flat plate with Moss et al.[40] and Li and Nagamatsu[37] results.

inviscid interactions on the flat plate and merges with the results of Li and Nagamatsu[37] within a few percentage points of difference in the aft part of the flat plate. Without viscous–inviscid interactions, the wall pressure remains equal to the freestream pressure. This additional pressure on the windward side of a slender body will give rise to significant lift. This phenomenon of viscous–inviscid interactions is not incorporated in the MINIVER,[11] the aeroheating,[12–14] or the INCHES[15] codes. Figure 4 shows a comparison of the results of skin-friction distribution on the flat plate from the present calculations with the DSMC results of Moss et al.[40] and the strong interaction results of Li and Nagamatsu.[37] As expected, the DSMC results of C_f differs quantitatively in the initial region of the flat plate from the corresponding HATLAP results. The peak volume from the two approaches differs by a few percent. In the strong interaction regime, the HATLAP results of C_f agree reasonably well with the corresponding DSMC results of Moss et al.[40] and Li and Nagamatsu[37] results. Figure 5 shows that the peak value of C_h by the present calculations is higher than the corresponding DSMC results of Moss et al.[40] by about 35% and the present results merge with the strong interaction results of Li and Nagamatsu[37] from about 0.75 cm to far downstream. The DSMC results of C_h from Moss et al.[40] are

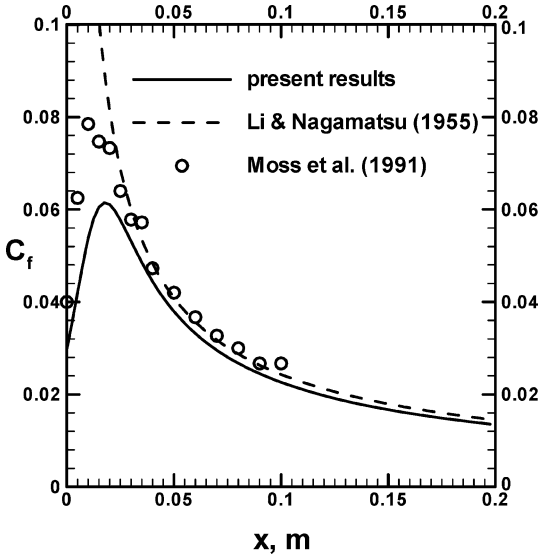

Fig. 4 Comparison of present results with viscous interactions on a sharp leading flat plate with Moss et al.[40] and Li and Nagamatsu[37] results.

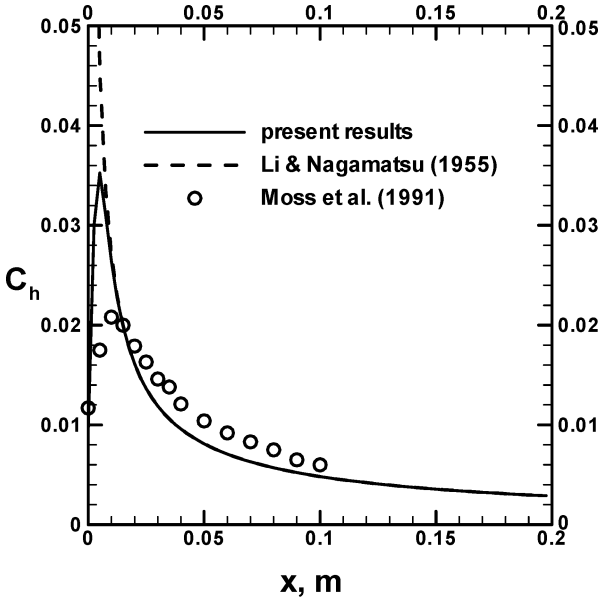

Fig. 5 Comparison of present results with viscous interactions on a sharp leading flat plate with Moss et al.[40] and Li and Nagamatsu[37] results.

higher than the Li and Nagamatsu[37] results and the present results in the strong interaction region by about 30% at 5 cm and 4% at 10 cm of the plate length. The discrepancy in C_f and C_h near the leading edge of the flat plate between the DSMC results of Moss et al.[40] and the present results may be attributed to different fluid mechanical models of flow in the two investigations and will have little effect in the overall aerodynamic and thermal coefficients.

Vidal et al.[42] carried out experiments in the Cornell Aeronautical Laboratory low-density wind tunnel for a flat plate at zero angle of attack under ambient conditions of $M_\infty = 24.0$, freestream Reynolds number per meter of 6.8×10^5, $\gamma = 1.4$, and $t_{w0} = 0.078$. The running length along the flat plate is taken as the characteristic length, and a linear viscosity–temperature law is used to calculate the freestream Reynolds number and the stagnation Reynolds number. Figure 6 presents a comparison of the results from the present calculations with the experimental data of Vidal et al.,[42] the strong interaction results of Li and Nagamatsu,[37] and free molecular results from Schaaf and Chambre.[34] The present results are in excellent agreement with the experimental data of Vidal et al.[42] and the strong interaction results of Li and Nagamatsu.[37] Note that the peak heating Stanton number from the present calculations agrees with the experimental data of Vidal et al.[42] and departs from the strong interaction theory of Li and Nagamatsu[37] to approach the free molecular limit, given by Schaaf and Chambre.[34]

Table 1 Comparison of coefficient p^* appearing in induced pressure; Eq. (9)

	p^*			
t_{w0}	Present calculation	HABP	Li and Nagamatsu[37]	Percent error in HABP
0.0	0.1216	0.1467	0.149	1.54
0.2	0.2110	0.2187	0.232	5.78
0.6	0.3497	0.3628	0.377	3.77
1.0	0.4884	0.5068	0.514	1.40

Table 2 Comparison of coefficient c^* appearing in skin-friction coefficient; Eq. (10)

	c^*			
t_{w0}	HATLAP	HABP	Li and Nagamatsu[37]	Percent error in HABP
0.0	0.1934	0.2543	0.208	−22.26
0.2	0.2568	0.3105	0.270	−15.00
0.6	0.3837	0.3999	0.412	+2.94
1.0	0.5105	0.4727	0.549	+13.92

Table 3 Comparison of coefficient s^* in Stanton number; Eq. (11)

	s^*			
t_{w0}	HATLAP	HABP	Li and Nagamatsu[37]	Percent error in HABP
0.0	0.0790	0.1272	0.0788	−62.06
0.2	0.1006	0.1552	——	——
0.6	0.1438	0.2000	0.155	−29.08
1.0	0.1870	0.2364	0.187	−26.42

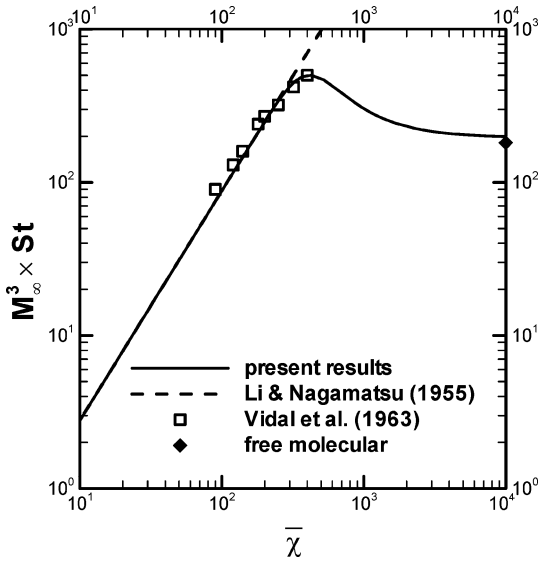

Fig. 6 Comparison of present results on a sharp-leading-edge flat plate with other theoretical[34,37] and experimental investigations.[42]

In Tables 1–3, a detailed comparison of the ratios of induced pressure due to viscous–inviscid interaction to freestream pressure, skin-friction coefficients, and Stanton numbers for different wall temperature ratios t_{w0} from the present calculations is made with the corresponding results from the HABP[10] code. In the HABP[10] code, analysis is based on the approach adopted by Bertram and Blackstock[16] and White.[17] Bertram and Blackstock[16] obtained similar solutions of the boundary-layer equations for induced pressure on

a flat plate at zero incidence and evaluated the effects of streamline curvature and leading-edge bluntness on the induced pressure. White[17] simplified the analysis for a sharp-leading-edge flat plate for engineering design purposes. Based on the work of White,[17] the induced pressure on a wedge is represented by the following expression:

$$P = p_w/p_\infty = P_0 + m \times \lambda \tag{4}$$

where

$$\lambda = a(t_{w0}, \gamma, Pr)$$

Here, P_0 is the ratio of inviscid pressure at the edge of the boundary layer on a wedge of semivertex angle α to freestream pressure, and m is a polynomial of fifth degree in $K_0 = M_\infty \sin\alpha$ (Ref. 10). For $\gamma = 1.4$ and $Pr = 0.72$, White[17] represented a by the following expression:

$$a = 0.07 + 0.17\, t_{w0} \tag{5}$$

To compare the results of the HABP code[10] with the Li and Nagamatsu[37] results and the present calculations, the following value of a is derived from the computed results of Li and Nagamatsu[37] for $\gamma = 1.4$ and $Pr = 1.0$:

$$a = 0.0733 + 0.1880\, t_{w0} \tag{6}$$

For the case of a flat plate at zero incidence, $P_0 = 1.0$, $m = 1.9156$, and

$$P = 1.0 + (0.1404 + 0.3601 t_{w0}) \times \bar{\chi} \tag{7}$$

White[17] suggested that

$$St = 2.0 \times C_f = 0.664\sqrt{PC/Re_{x\infty}} \tag{8}$$

Equation (8) is one of the several formulations used to evaluate Stanton number St and C_f for flows with pressure gradients in the HABP code.[10] From Eqs. (4–8), the following expressions for flat plate at zero incidence can be derived:

$$P = p_w/p_\infty = p^* \times \sqrt{\bar{\chi} C/Re_{x\infty}} \tag{9}$$

$$C_f = c^* \times \sqrt{\bar{\chi} C/Re_{x\infty}} \tag{10}$$

$$St = s^* \times \sqrt{\bar{\chi} C/Re_{x\infty}} \tag{11}$$

Values of p^*, c^*, and s^* for $\gamma = 1.4$ and $Pr = 1$ from the present calculations, Li and Nagamatsu,[37] and HABP[10] results as modified in the manner stated earlier are presented in Tables 1–3. Observe from Tables 1–3 that, in comparison to the results of Li and Nagamatsu,[37] the maximum difference in p^*, c^*, and s^* in the present calculations is less than 10, 7 and 1%, respectively, and the corresponding results from the HABP code differ by less than 6, 22 and 62%, respectively. Note that the difference in Stanton number in the HABP[10] code from the present calculations is highest when the wall temperature is lowest. This is generally the situation that a space vehicle encounters flying under hypersonic conditions. The Stanton number variation with Reynolds number at $t_{w0} = 0.0$ from the present method, Li and Nagamatsu,[37] and HABP,[10] methods is shown in Fig. 7. It can be concluded that the engineering predictions of C_p, C_f, and Stanton number St from the present calculations are well within the acceptable limits, whereas the prediction of C_p from the HABP code are within the acceptable limits but the predictions of C_f and particularly Stanton number St are not acceptable for design purposes. The differences in C_h on wedges may be significantly more than on flat plates.

The shuttle reenters the atmosphere at an angle of 40 deg with the freestream. Dogra and Moss[43] approximated the wing mean chord of the shuttle with a flat plate 12 m long. They investigated the flowfield and surface quantities with the DSMC method for a flat plate 12 m long, inclined at an angle of 40 deg with the freestream

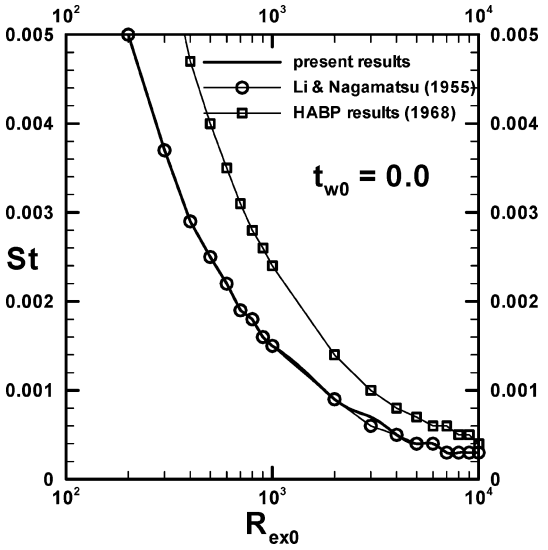

Fig. 7 Comparison of present result with viscous interactions on a sharp-leading-edge flat plate with other theoretical investigations.[10,37]

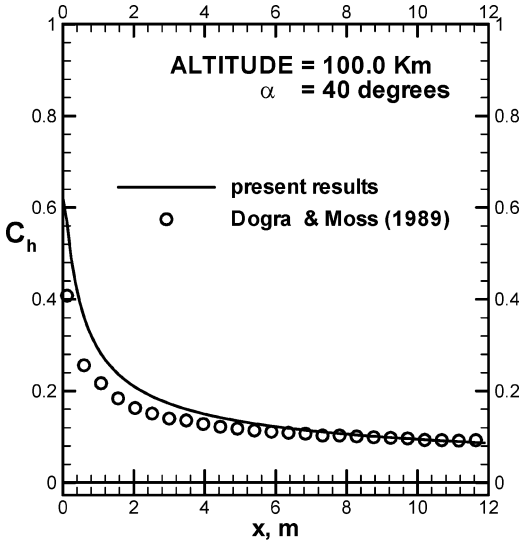

Fig. 8 Comparison of present results on the flat plate with Dogra and Moss[43] results.

as it traverses the atmosphere from 200 to 100 km with a constant velocity of 7.5 km/s. Parametric studies were carried out with respect to the angle of attack and wall temperature. The purpose of the investigation was to study the effect of rarefaction on flowfield and surface quantities in the transitional regime.

A detailed comparison of C_h on the 12-m-long flat plate at 40-deg angle of attack under the shuttle flight conditions from 70 to 200 km from the present calculations with the corresponding results of Dogra and Moss[43] is given by Jain.[44] Here, the effectiveness of the present method in the transitional regime is shown. In Fig. 8, comparison of the present results of C_h on the flat plate with the corresponding DSMC results of Dogra and Moss[43] under 100-km shuttle flight conditions show slight departure of the DSMC results in the initial region of the flat plate. In the aft portion of the flat plate, the two results merge with each other. The differences in the initial region of the flat plate may be due to the different models of flow adopted in the two approaches. In Fig. 9, comparison of our results for C_h with the DSMC results on the flat plate inclined at 20, 40, 60, and 80 deg with the freestream under shuttle flight conditions of 160 km is shown. In all cases, the agreement of the present calculations with the DSMC results is reasonably good. In Fig. 10, agreement of the present results and the experimental data by Vidal

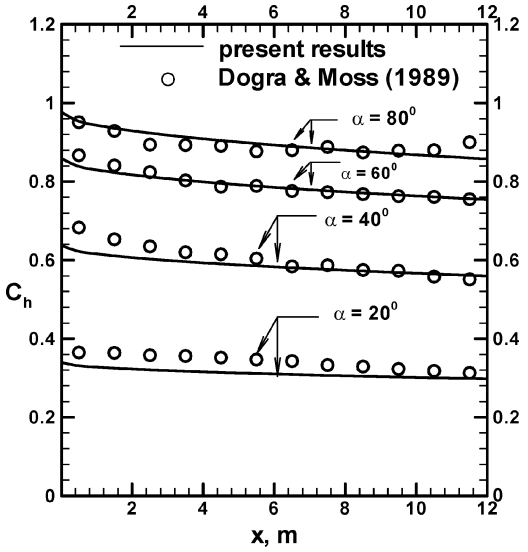

Fig. 9 Comparison of present results on the flat plate at various angles of attack under 160-km shuttle flight conditions with Dogra and Moss[43] results.

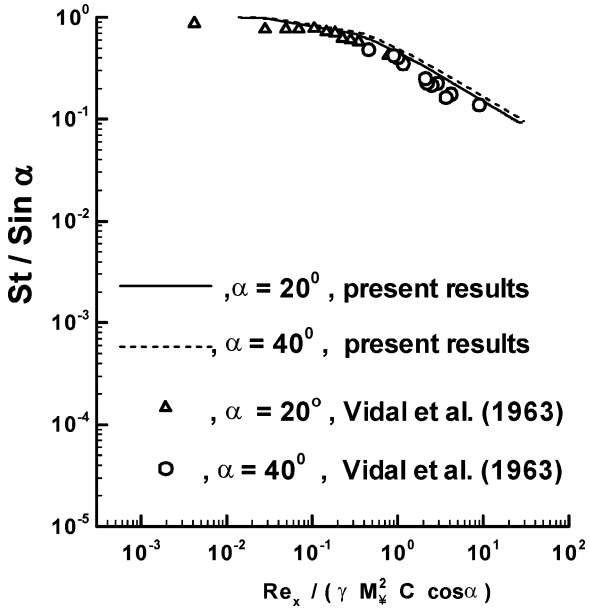

Fig. 10 Comparison of present results on wedges with corresponding Vidal et al.[42] experimental data.

et al.[42] on wedges of semivertex angles of 20 and 40 deg is good. Here, c is the modified Chapman and Rubesin constant defined as follows:

$$c = \left[\mu(T^*)\big/\mu(T_\infty)\right] \times T_\infty \big/ T^* \tag{12}$$

$$T^*\big/T_{\text{wall}} = T_{\text{wall}}/T_{e0} + \tfrac{1}{2}(1 - T_{\text{wall}}/T_{e0}) - \tfrac{1}{3}\cos^2\alpha \tag{13}$$

with α being the semivertex angle of the wedge.

Conclusions

The basic approach to develop a new generic engineering HATLAP method that predicts surface quantity (pressure, skin-friction, and heat transfer) distributions on a vehicle of arbitrary shape is explained and is validated on planar bodies for flow conditions in hypersonic continuum, transitional, and free molecular flow regimes. Contributions of induced pressure due to viscous–inviscid interactions in the hypersonic flight regime are found to be significant enough to affect the performance qualities of the vehicle. HABP,[10] is the only engineering code that includes the induced pressure prediction capability. HABP,[10] prediction of induced pressure is reasonably good, but heating predictions are considerably higher than the present results from the HATLAP method and the Li and Nagamatsu[37] results, particularly at low wall temperatures. The available engineering codes (MINIVER,[11] aeroheating,[12–14] and INCHES[15]) do not predict surface quantities with induced pressure effects. Considerable experience is needed in running these codes. In contrast, the HATLAP method provides unique results of surface quantities (C_p, C_f, and C_h) on bodies of different shape, is easy to execute, and is highly accurate. In the companion paper, validation of the HATLAP methodology on three-dimensional bodies will be carried out.

Acknowledgments

The work was performed under Contract F33615-97-C-3000 from the U.S. Air Force Research Laboratory, Wright–Patterson Air Force Base, Ohio, as part of Small Business Innovation Research Phase I efforts. A. C. Jain thanks J. N. Moss of NASA Langley Research Center, Hampton, Virginia, for technical discussions and for providing digitalized data of direct simulation Monte Carlo calculations presented in this report.

References

[1]Jain, A. C., *Lectures on Reentry Aerodynamics*, Vikram Sarabhai Space Center, Trivandrum, India, 1980.

[2]Jain, A. C., and Dahm, W., "Hypersonic Merged Layer Blunt Body Flows with Wakes," *Proceedings of the 17th International Symposium on Rarefied Gas Dynamics*, edited by A. E. Beylich, VCH, New York, 1990, pp. 578–587.

[3]Jain, A. C., and Adimurthy, V., "Hypersonic Merged Layer Flows, Part 1: Adiabatic Wall Case," *AIAA Journal*, Vol. 12, No. 3, 1974, pp. 342–347.

[4]Jain, A. C., and Adimurthy, V., "Hypersonic Merged Layer Flows, Part 2: Cold Wall Case," *AIAA Journal*, Vol. 12, No. 3, 1974, pp. 348–354.

[5]Jain, A. C., "Hypersonic Merged Layer Flow on a Sphere," *Journal of Thermophysics and Heat Transfer*, Vol. 1, No. 1, 1985, pp. 21–27.

[6]Jain, A. C., and Kumar, A., "Nonequilibrium Merged Stagnation Shock Layers at Hypersonic Speeds," *International Journal of Heat and Mass Transfer*, Vol. 18, 1975, pp. 1113–1118.

[7]Jain, A. C., and Kumar, P., "An Improved Stagnation Point Viscous Shock-Layer Flow over a Blunt Body," *Proceedings of the 15th International Symposium on Rarefied Gas Dynamics*, edited by V. Boffi and C. Cercignani, B. G. Teubner, Stuttgart, Germany, 1986, pp. 597–606.

[8]Jain, A. C., and Prabha, S., "A Comparative Study of Stagnation Point Viscous Shock Layer and Hypersonic Merged Layer Flows," *Proceedings of the 14th International Symposium on Rarefied Gas Dynamics*, edited by H. Oguchi, Univ. of Tokyo, Tokyo, 1984, pp. 241–248.

[9]Potter, J. L., and Peterson, S. W., "Local and Overall Aerodynamic Coefficients for Bodies in Hypersonic, Rarefied Flow," AIAA Paper 91-0336, Jan. 1991.

[10]Gentry, A. E., and Smyth, D. N., "Hypersonic Arbitrary-Body Aerodynamic Computer Program (Mark III Version) Vol. II: Program Formulations and Listings," McDonnell Douglas Aeronautics Co., Doughpal Rept. DAC 61442, St. Louis, MO, April 1968.

[11]Engel, C., and Praharaj, S. C., "Miniver Upgrade for the AVID System," *LANMIN Users Manual*, Vol. 1, NASA CR 172212, Aug. 1983.

[12]Fivel, H. J., "Numerical Flow Field Program for Aerodynamic Heating Analysis," *Equations and Results*, Vol. 1, Air Force Flight Dynamics Lab., Rept. AFFDL-TR-79-3128, Wright–Patterson AFB, OH, Dec. 1979.

[13]DeJarnette, F. R., and Davis, R. M., "A Simplified Method of Calculating Laminar Heat Transfer over Bodies at an Angle of Attack," NASA TN-4720, Aug. 1968.

[14]Hamilton, H., DeJarnette, F. R., and Weilmuenster, K. J., "Application of Axisymmetric Analogue for Calculating Heating Rates in Three-Dimensional Flows," *Journal of Spacecraft and Rockets*, Vol. 24, No. 4, 1987, pp. 296–303.

[15]Zoby, E. V., and Simmonds, A. L., "Engineering Flowfield Method with Angle-of-Attack Applications," *Journal of Spacecraft and Rockets*, Vol. 22, No. 4, 1985, pp. 398–404.

[16]Bertram, M. H., and Blackstock, T. A., "Some Simple Solutions to the Problem of Predicting Boundary Layer Self-Induced Pressures," NASA TN D-798, April 1961.

[17]White, F. M., Jr., "Hypersonic Laminar Viscous Interactions on Inclined Flat Plates," *ARS Journal*, Vol. 32, May 1962, pp. 780, 781.

[18]Wurster, K., Zoby, E., and Thompson, R., "Influence of Flow Field and Vehicle Parameters on Engineering Aerothermal Methods," AIAA Paper 89-1769, June 1989.

[19]Lewis, A. B., Jr., and Sliski, N. J., "Investigation of Numerical Techniques for Predicting Aerodynamic Heating to Flight Vehicles," U.S. Air Force Flight Dynamics Lab., Rept. AD-A079121/AFFDL-TR-79-3001, Wright–Patterson AFB, OH, May 1979.

[20]Cooke, J. C., "An Axially Symmetric Analogue For General Three-Dimensional Boundary Layers," British Aeronautical Research Council, Rept. and Memorandum No. 3200, London, 1961.

[21]Beckwith, I. E., and Cohen, N. B., "Application of Similar Solutions to Calculation of Laminar Heat Transfer on Bodies with Yaw and Large Pressure Gradient in High Speed Flow," NASA TN D-625, 1961.

[22]Reshotko, E., and Tucker, M., "Approximate Calculation of the Compressible Boundary Layer with Heat Transfer and Arbitrary Pressure Gradient," NASA TN 4154, Dec. 1957.

[23]Maslen, S. H., "Inviscid Hypersonic Flow past Smooth Symmetric Bodies," *AIAA Journal*, Vol. 2, No. 6, 1964, pp. 1055–1061.

[24]Thompson, R. A., Zoby, E. V., Wurster, K. E., and Gnoffo, P. A., "An Aerothermodynamic Study of Slender Conical Vehicles," AIAA Paper 87-1475, June 1987.

[25]Jain, A. C., "Mathematical Formulation for Predicting Pressure, Skin-friction, Heat Transfer Distributions on Vehicles of Arbitrary Shape," Science and Technology Corp., STC TR 3313, Hampton, VA, March 2003.

[26]Bird, G. A., "Monte Carlo Simulation in an Engineering Context," *Rarefied Gas Dynamics*, edited by S. Fisher, Vol. 74, Pt. 1, Progress in Astronautics and Aeronautics, AIAA, New York, 1981, pp. 239–255.

[27]Gupta, R. N., Lee, K. P., Thompson, R. A., and Yos, J. M., "Calculations and Curve-Fits of Thermodynamics and Transport Properties for Equilibrium Air to 30000K," NASA RP 1260, Oct. 1991.

[28]Hansen, C. F., "Approximations for Thermodynamic and Transport Properties of High Temperature Air," NASA TR-R50 (supersedes NACA TN 4150), Nov. 1957.

[29]Jain, A. C., and Li, T. Y., "Problem of Sharp Leading Edge in Hypersonic Flow," Aeronautical Research Lab., ARL Rept. 63-161, Wright–Patterson AFB, OH, 1961.

[30]Kumar, A., and Jain, A. C., "Hypersonic Viscous Slip Flow past Insulated Wedges," *AIAA Journal*, Vol. 10, No. 8, 1972, pp. 1081–1083.

[31]Jain, A. C., and Kumar, A., "Hypersonic Rarefied Flow past an Insulated Flat Plate with Suction/Injection," *International Journal of Heat and Mass Transfer*, Vol. 15, Dec. 1972, pp. 2401–2407.

[32]Chaudhury, P., "Hypersonic Rarefied Viscous–Inviscid Interaction on Insulated Wedges," M. Technology Thesis, Dept. of Aerospace Engineering, Indian Inst. of Technology, Kanpur, India, May 1978.

[33]Mathews, V. K., "Hypersonic Viscous Slip Flow past Non-Insulated Wedges," M. Technology Thesis, Dept. of Aerospace Engineering, Indian Inst. of Technology, Kanpur, India, Dec. 1978.

[34]Schaaf, S. A., and Chambre, P. A., *Flow of Rarefied Gases*, Princeton Univ. Press, Princeton, NJ, 1961, pp. 8–24.

[35]Katov, V. M., Lychkin, E. N., Reshetin, A. G., and Scheikonogov, A. N., "An Approximate Method of Aerodynamics Calculation of Complex Shape Bodies in a Transition Region," *Proceedings of the 13th International Symposium on Rarefied Gas Dynamics*, Vol. 1, edited by O. M. Belotserkivskii et al., Plenum, New York, 1982, pp. 487–494.

[36]Knox, E. C., and Jain, A. C., "Technical Summary of Improved Aerodynamic Bridging Procedures," NASA Contract NAS8-38416, REMTECH RTR 211-01, Aug. 1992.

[37]Li, T. Y., and Nagamatsu, H. T., "Hypersonic Viscous Flow on Noninsulated Flat Plate," *Proceedings of the 4th Midwestern Conference on Fluid Mechanics*, Purdue Univ., Lafayette, IN, 1955, pp. 273–287.

[38]Knox, E. C., Jain, A. C., and Seaford, C. M., "Hypersonic Viscous Aerodynamics Using Improved Bridging Procedures," AIAA Paper 93-3445, Aug. 1993.

[39]Merski, R., "Thermophysics," *Aerospace America*, Dec. 2002, pp. 22, 23.

[40]Moss, J. N., Price, J. M., and Chun, C.-H., "Hypersonic Rarefied Flow About a Compression Corner-DSMC Simulation and Experiment," AIAA Paper 91-1313, June 1991.

[41]Bertram, M. H., and Feller, W. V., "A Simple Method for Determining Heat Transfer, Skin-Friction, and Boundary Layer Thickness for Hypersonic Laminar Boundary Layer Blows in Pressure Gradient," NASA Memo 5-24-59L, June 1959.

[42]Vidal, R. J., Golian, T. C., and Bartz, J. A., "An Experimental Study of Hypersonic Low-Density Viscous Effects on a Sharp Flat Plate," Cornell Aeronautical Lab., CAL Rept. 63-435, Buffalo, NY, Aug. 1963; also Rept. A63-20607, 1963.

[43]Dogra, V. K., and Moss, J. N., "Hypersonic Rarefied Flow About Plates at Incidence," AIAA Paper 89-1712, June 1989.

[44]Jain, A. C., "Hypersonic Aerothermal Analysis Program for a Maneuvering Missile/Fighter Aircraft," Science and Technology Corp., STC TR 3163, Hampton, VA, Jan. 1998.

C. Kaplan
Associate Editor